Corrosion Science 94 (2015) 179–189

Contents lists available at ScienceDirect

Corrosion Science

journal homepage: www.elsevier.com/locate/corsci

Investigation of the effect of solution annealing temperature on critical pitting temperature of 2205 duplex stainless steel by measuring pit solution chemistry

M. Naghizadeh, M.H. Moayed *

Metallurgical and Material Engineering Department, Faculty of Engineering, Ferdowsi University of Mashhad, Mashhad 91775-1111, Iran

ARTICLE INFO

Article history:
Received 22 August 2014
Accepted 30 January 2015
Available online 4 February 2015

Keywords:
A. Stainless steel
B. Polarisation
C. Anodic dissolution
C. Pitting corrosion

ABSTRACT

In this research, the effect of solution annealing temperature on critical pitting temperature of DSS 2205 in 3.5 wt.% NaCl solution and also the pit chemistry is studied using electrochemical methods and mechanistic analyses. Pencil electrode studies revealed that in comparison to samples solution annealed at 1050 °C and 1150 °C, maximum current density in simulated pit solution is increased and limiting current density in presence of salt film is decreased for alloy solution annealed at 1250 °C. Based on these results and microscopic observations, lower CPT of DSS 2205 solution annealed at 1250 °C is explained.

1. Introduction

Pitting corrosion is one of the most intensive types of localised corrosion which have received considerable attention in the literature [1–10]. It is known that pitting corrosion occurs in three consecutive stages including pit initiation, metastable pitting and stable pit growth [11]. Earlier works [1,10,12–17] have accounted the presence of salt film at the bottom of dissolving pit to be a required factor for sustaining pit growth. In this stage, the dissolution rate is controlled by diffusion of metal cations through the salt [12] and is independent of applied potential [16,18]. Considering Fick's first law, diffusion controlled limiting current density is calculated as below:

$$i_{\lim} = \frac{n \cdot F \cdot D \cdot C_S}{\delta} \quad (1)$$

where $i_{\lim}$ is limiting current density, δ is pit depth, and C_S is metal cation saturation concentration essential for the metal salt to precipitate at the pit bottom. Other characters namely n, F, and D, are metal cations valance, Faraday's constant and metal cations diffusivity, respectively [16].

Investigations on the composition of metal salt precipitated at the bottom of pits formed on the surface of Fe–Cr–Ni stainless steels in chloride solutions have revealed that $FeCl_2$ is the major constituent of the salt film [19], while chloride salts of other elements except Mo [20] are also presented in their stoichiometric proportion existed in the bulk alloy [18].

One of the factors used for ranking the resistance of stainless steels to pitting corrosion is the critical pitting temperature (CPT) below which stable pitting does not take place [21,22]. Because of the large applications of duplex stainless steels (DSSs) in marine and petrochemical industries, the CPT of this type of stainless steels has been widely investigated [23–27]. Duplex stainless steels are high pitting resistance alloys which comprise ferrite and austenite simultaneously and contain high amount of key elements in corrosion resistance (Cr, Mo and N) [28]. To offer the favourable properties, this type of stainless steel is mainly solution annealed at a temperature above 1000 °C. Solution annealing at these temperatures yield a microstructure free of isothermal secondary phases [29]. Since subjecting to thermal cycles like welding could change ferrite/austenite phase fraction and also may lead to microstructural alterations, many investigations have been conducted on the influence of annealing temperature on CPT of duplex stainless steels [25,30]. Investigating the chemical composition of phases in different annealing conditions, several researchers have related the CPT to the PREN (pitting resistance equivalent number) of weakest phase [23,30–32], which itself is related to the content of three most essential elements, i.e. Cr, Mo and N [33,34]. Some literature have related the CPT of DSSs to the influence of precipitation of chromium nitride as the secondary phase formed in the microstructure during the solution annealing heat treatments through the fast cooling from higher temperatures [25,35–39]. It is believed that the deleterious effect of chromium nitride on

* Corresponding author. Tel./fax: +98 511 8763305.
E-mail address: mhmoayed@um.ac.ir (M.H. Moayed).

http://dx.doi.org/10.1016/j.corsci.2015.01.051
0010-938X/

localised corrosion of duplex stainless steels is due to the depletion of Cr from proximity of precipitations [40].

The large number of evidences suggest that pitting corrosion is controlled by factors relating to pit growth stability [41] and CPT is defined as a temperature below which transition from metastable to stable pitting could not be occurred at any potential [42,43]. Many researchers have investigated stable dissolution kinetic of pits by means of pencil electrodes to gain a better understanding of a single pit growth [12,14–16,44]. They used pencil electrode technique to create a single pit and avoid random pits occurrence on the investigated surface. Salinas-Bravo and Newman [45] suggested a new method of measuring CPT based on inability of metal to dissolve with sufficiently high rate to supply a localised chemistry. They introduced CPT as a temperature at which the limiting current density at the presence of salt film at the pit bottom (i_{lim}) and the maximum current density before passivation (i_{max}) have the same values. According to this CPT definition, at temperatures below CPT, due to occurrence of passivity, the local concentration of aggressive anions could not be supplied at the pit. At temperatures above CPT, salt film precipitation prohibits necessary conditions for passivation and pit could be sustained [46].

Moayed [47] employed pencil electrode method to investigate the correlation between CPT of 904L SS and pit solution in presence of sulphate ion. Addition of sulphate has found to have a detrimental effect on CPT. Their investigation revealed that addition of sulphate decreases the saturated concentration of metal cations (C_S) within the pit solution. Lately, using 50 μm pencil electrode, it is shown that thiosulphate has the same effect on the saturation concentration of metal cations within the pit solution in 316 stainless steel [48]. Recently, Zakeri and Moayed [49] studied the effect of nitrate ion on CPT of DSS 2205 using 80 μm pencil electrode. They demonstrated that, in presence of nitrate ion, limiting current density in presence of salt film increases and the maximum current density decreases, which lead to an improve in CPT. The effect of different anions on the pit chemistry [47–52] and also the effect of solution annealing temperature on the PREN and their correlation with CPT [23,25,30,36,39,53,54] were extensively investigated. However, the effect of microstructural alteration on the pit chemistry and its corresponding effect on the critical pitting temperature (CPT) has not yet been studied.

In the present work, first the effect of annealing temperature on CPT of DSS 2205 was assessed in 3.5 wt.% NaCl solution using potentiodynamic and potentiostatic polarisation methods. Then, the influence of microstructural changes on the CPT was studied using 2205 DSS pencil electrode based on the mechanistic point of view that how a change in the maximum current density and the limiting current density may lead to a shift in CPT. For this purpose, the saturation concentration of metal cations was assessed for alloy solution annealed at 1050 °C and 1250 °C. After that, the anodic dissolution of solution annealed samples was evaluated by potentiodynamic polarisation of samples in simulated pit solution. The investigation on the effect of solution annealing temperature on the PRE number of DSS 2205 was not interested in this research.

2. Experimental procedure

2.1. Materials and electrode preparation

For all electrochemical investigations and metallographic examinations, UNS S32205 duplex stainless steel supplied in wrought form, was used. The alloy composition was as listed in Table 1. To measure CPT, rod-shaped samples were machined from a thick plate, then were solution annealed at 1050 °C, 1150 °C and 1250 °C for 45 min, afterwards water quenched immediately. To make the electrical connection, the other end of each bullet electrode was connected to a shielded copper wire which was inserted into a rigid plastic tube. Before each test, working electrode was ground from 60 to a 1200 grit finish and then rinsed with deionised water followed by drying with warm air. After each test, precise inspections were performed using a stereo microscope to confirm that only definite pitting was occurring. The immersed surface of working electrodes was at least 4 cm^2.

In mechanistic studies, pencil electrode technique was employed. Pencil electrodes were prepared by drawing the wires (with 0.4×0.4 mm^2 square cross section) cut from the bar into 250 μm diameter wires. After that, samples were solution annealed at 1050 °C and 1250 °C for 30 min and water quenched. Afterwards, 200 μm dia. and also 80 μm dia. pencil electrodes were prepared by electropolishing the 250 μm dia. wires in 70% phosphoric acid solution to study the effect of solution annealing temperature on i_{max} and i_{lim}, respectively. The wire specimens were mounted in an epoxy resin with one cross-sectional surface exposed to 3.5 wt.% chloride solution. Before each test, the exposed surface was ground to 60 grit to increase the probability of pit initiation at more occluded sites [46], then rinsed with deionised water and finally dried with warm air.

For microscopic observations, 10 mm × 10 mm flat samples were prepared. The heat treatment process was the same as what applied for rod-shaped samples. Then, grinding was performed using silicon carbide papers of 60–2000 grit size and specimens were electro-etched in 20 N KOH etching solution at 2 V for 10 s after being polished by 0.3 μm alumina paste. Image analysis was applied using MIP™ software to quantify the effect of solution annealing temperature on the phase fraction of austenite and ferrite phases. Further metallographic examination was performed after electro-etching in glyceregia reagent which darkens secondary phases like carbide and nitride [55]. Identification of the secondary phase in sample solution annealed at 1250 °C was performed using a field emission secondary electron microscope equipped with energy-dispersive X-ray spectrometer (EDS). For this purpose, sample were polished, electro-etched in 40% HNO_3 at 1 V for 2 min, and then at 0.75 V for 7 min [56].

2.2. Electrochemical procedures

All electrochemical polarisation experiments were conducted using a Gill AC automated potentiostat (ACM Instruments). The solutions were prepared with deionised water and analytical grade chemicals. Electrochemical cells were composed of platinum counter electrode and a saturated calomel electrode (SCE) as a reference electrode. All potentials quoted in this work refer to SCE. Before each test, the sample was allowed to stabilise at open-circuit potential in investigated solution.

Critical pitting temperature evaluations on DSS 2205 solution annealed at different temperatures, were performed in 3.5 wt.% NaCl medium. The pure nitrogen gas (N_2) was purged into the test solution from 30 min before starting each test and was continued during the test at the top of the solution. Potentiodynamic polarisation measurements were conducted at temperatures between 25 °C and 75 °C with 10 °C intervals by sweeping the potential from 50 mV below the rest potential, at a given scan rate (0.5 mV s^{-1}) till the current density exceeded 300 μA cm^{-2}. The potential at which current density began to increase, was considered as the breakdown potential (E_b) [46]. The temperature at which the value of E_b decreased dramatically, considered as the CPT [26,46,56]. Potentiostatic polarisation method used for CPT determination was involved polarisation of sample at 650 mV (SCE) in the 3.5 wt.% chloride solution and increasing the solution temperature at a rate of 0.6 °C min^{-1}. Each test continued until the current density exceeded 200 μA cm^{-2} and temperature at which current density begins to increase, was considered as the CPT [46]. Each test was repeated at least three times to ensure reproducibility of data.

Table 1
Chemical composition of experimented DSS 2205.

Element	C	Cr	Ni	Mo	V	P	W	Mn	Si	N	Fe
wt.%	0.023	21.6	5.3	3.1	0.136	0.02	0.064	1.18	0.5	0.15	Bal.

For creating a single corrosion pit and measuring the current density associated with individual pit, 80 μm dia. pencil electrodes were exposed to the medium with face upward to avoid venting of precipitated salt. Then, electrodes were potentiostatically polarised at 850 mV (SCE) in 3.5 wt.% NaCl solution at 65 °C. After that, potential was ramped to the passive region potentiodynamically at a sweep rate of 1 mV s^{-1}. Because of low probability of pit initiation at temperatures close to the CPT due to small size of the specimen [57], test temperature and potential was selected greatly above the CPT and pitting potential that was obtained for DSS 2205. Since we had to consider the same pit depth for each single pit created in pencil electrode studies, and because the pit depth is dependent on the charge flows during the formation of single pit in the initial times of the experiment; so, it is impossible to create single pits with the exact same pit depth. To eliminate the effect of pit depth, we created the pits with a depth in the range of 540–720 μm.

Finally, maximum current density at various temperatures was assessed by means of potentiodynamic polarisation test using 200 μm dia. pencil electrodes in 5 M HCl solution as the simulated pit solution [58]. The specimens were placed in an electrochemical cell with the exposed faces upwards. After obtaining stable condition, polarisation curves were recorded at a sweep rate of 5 mV s^{-1}. Each test was repeated 5 times under the identical conditions.

3. Experimental results

3.1. Morphology observation analysis

A microscopic inspection of steel solution annealed at various temperatures was undertaken to find some clues to the outcome of solution annealing treatment temperatures on the microstructural features. Fig. 1 shows the microstructure obtained from DSS 2205 solution treated at 1050 °C, 1150 °C and 1250 °C. The microstructures show austenite islands (white region) in a continuous ferrite matrix (grey region) [23,59]. As observed, a progressive increase in ferrite phase volume fraction occurs as solution annealing temperature increases. Image analysis conducted using MIP™, revealed that ferrite fraction increases from 46% in sample solution annealed at 1050 °C to 55% and 68% for samples solution annealed at 1150 °C and 1250 °C, respectively. To investigate whether any secondary phase exists in the microstructures, specimens were etched with glyceregia etchant, which darkens the secondary phases like carbide and nitride [55]. As it is clear in Fig. 2a and b, there is no evidence of secondary phase precipitation in the microstructure of specimens that were solution annealed at 1050 °C and 1150 °C. However, precipitations appear as dark specks in the micrograph of sample quenched from 1250 °C. This secondary phase is observed mainly in the interior of ferrite region with some distance from austenite grains (see Fig. 2c).

The Fe-SEM image of this phase is shown in Fig 3a. The result of analysis of the composition of the black needles and the ferritic matrix by energy dispersive spectroscope (EDS) connected to the Fe-SEM are shown in Fig. 3b and c.

3.2. Effect of annealing temperature on the CPT

3.2.1. Potentiodynamic polarisation

Fig. 4 shows the potentiodynamic polarisation results of solution annealed DSS 2205 samples in 3.5 wt.% NaCl solution at different temperatures. It can be seen that pitting corrosion potential (E_{pit}) and the passivity region of alloy in all annealing conditions decreases with increase in test temperature.

The plots of breakdown potential (E_b) vs. temperature, obtained from polarisation curves are illustrated in Fig. 5. It is obvious that the breakdown potentials of specimen solution annealed at 1050 °C and one solution annealed at 1150 °C range from ca. 1100 mV (SCE) to ca. 1020 mV (SCE) at temperatures between 25 °C and 45 °C. By increasing the solution temperature above 45 °C, the breakdown potentials continue to decrease. At 55 °C, the value of E_b of sample solution annealed at 1050 °C and one solution annealed at 1150 °C decreases to ca. 715 mV (SCE) and ca. 680 mV (SCE), respectively. The sudden drop in E_b values at temperatures between 45 °C and 55 °C indicates that, for samples solution annealed at 1050 °C and one solution annealed at 1150 °C, transition from transpassivity to pitting corrosion takes place at this temperature range (not necessarily at the same temperature). It is shown in Fig. 5 that breakdown potential of alloy solution annealed at 1250 °C, decreases from ca. 1075 at 35 °C to ca. 750 mV (SCE) at 45 °C. Thus, it can be concluded that pitting corrosion occurs at a temperature between 35 °C and 45 °C. By increasing the temperature, breakdown potential of alloy solution annealed at 1250 °C decreased to ca. 490 mV (SCE), 290 mV (SCE) and 210 mV (SCE) at temperatures of 55 °C, 65 °C, and 75 °C, respectively. At temperatures above 45 °C, the breakdown potential of sample solution annealed at 1250 °C is obviously lower compared to two other specimens. In summary, based on potentiodynamic measurements at various temperatures (see Figs. 4 and 5), subjecting the specimen at 1150 °C causes no significant change in the pitting potential compared to solution annealing at 1050 °C. whilst, it is evident that solution annealing at 1250 °C leads to a decrease in breakdown potential in comparison to other examined solution annealing conditions and solution annealing at 1250 °C decreases the CPT to a value between 35 °C and 45 °C.

3.2.2. Potentiostatic polarisation with rising temperature

Fig. 6 represents a typical current density vs. temperature curves obtained from potentiostatic CPT assessment for DSS 2205 solution annealed at various temperatures in 3.5 wt.% NaCl solution. Metastable current transients providing information on the initiation stage of pitting corrosion were observed in lower temperature for specimen solution annealed at 1250 °C when compared to other solution annealed samples. The temperature at which current density begins to increase (the temperature associated with the onset of stable pitting) was considered as CPT. As observed, the critical pitting temperature of specimens solution annealed at 1050 °C and 1150 °C are around 58 °C. The CPT of sample solution annealed at 1250 °C is approximately 51 °C that is 7 °C lower in comparison with the CPT of other solution annealed specimens.

3.3. Pencil electrode studies

3.3.1. Under salt film dissolution behaviour

Pencil electrode studies were performed to assess the effect of solution annealing temperature on the chemistry of pit solution and pit propagation stage. This experiment was involved two consecutive steps. Fig. 7 illustrates a typical current density response of alloy in 3.5 wt.% NaCl solution at 65 °C to the potentiostatic polarisation at a constant potential of 850 mV (SCE) and also potentiodynamic polarisation to the passive region with sweeping rate of 1 mV s^{-1}. At the initial part of the first step, curve shows a

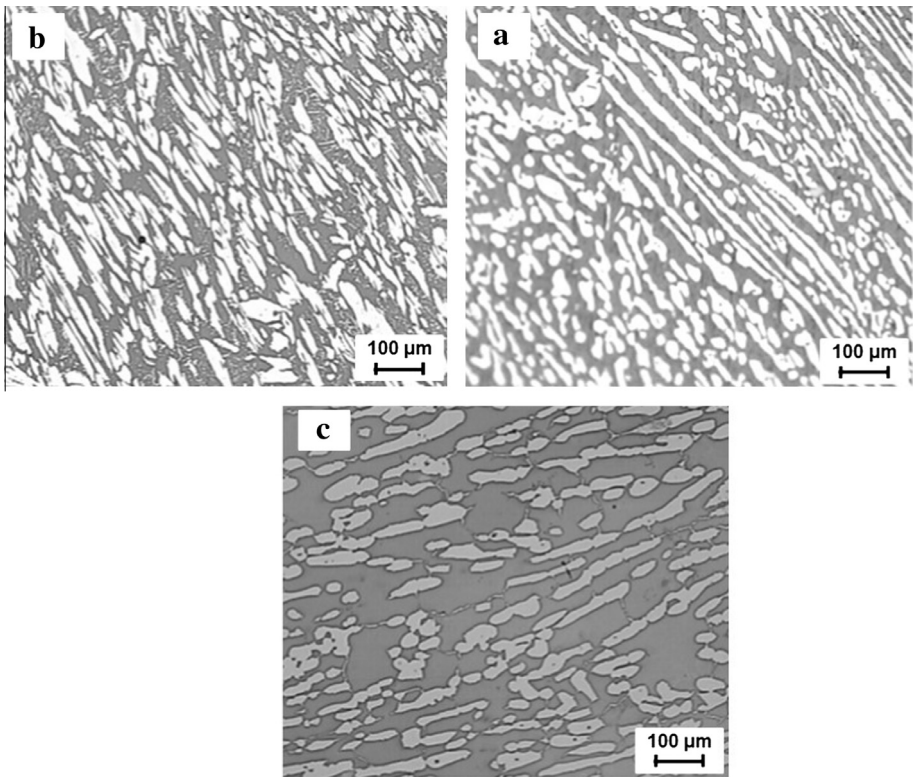

Fig. 1. Optical micrographs of DSS 2205 solution annealed at (a) 1050 °C, (b) 1150 °C, and (c) 1250 °C, etched in KOH, showing ferrite (dark region) and austenite (bright region) phase.

sharp spike due to the formation and the coalescence of stable pits followed by a decrease in the current density and then a plateau region [60]. It should be noted that polarisation data with nonstandard shape or which represented a deviation from Fick's first law or include an extremely noisy current density–time part were not used for analysis. It also worth noting that fluctuations observed in the plateau region, are real and reproducible and could be attributed to the local activation and repassivation under the salt layer [60].

The proportion of current density with time seems to be under diffusional control, similar to those reported by Tester and Isaacs [16]. Neglecting the migration and convection parts of mass transport, pit depth (δ) (the depth of which embedded wire has dissolved) was calculated using Eq. (2) by measuring the total charge passed during the curve of current density vs. time [13].

$$\delta = \frac{M_w}{n \cdot F \cdot \rho} \int i \cdot dt \tag{2}$$

Making the assumption that the metal components of the alloy are oxidised to Fe^{2+}, Cr^{3+}, and Ni^{2+} during dissolution, it is thus justified to assume that the mean value of oxidation state of cations (n), average atomic weight (M_w), and average atomic density (ρ) are 2.23, 55.2 g, and 7.87 g cm^{-3}, respectively.

After holding the electrode at the potential of 850 mV (SCE) and growing the pit for a given time (shown as step 1 in Fig. 7), diffusion limiting current density was measured by reverse scanning of potential to the potential at which passivity could be established again. Considering step 2 in Fig. 7, ramping the potential from point (a) to the lower values does not change the current density relation with time, which is an indication of the fact that pit still grows under the diffusion control at the presence of salt film [12]. However, reducing the potential causes salt film thickness to decrease in this region [61]. Once the potential reaches to the value which cation concentration reaches below the saturated concentration (C_S), precipitated salt would not be longer stable. Thereby, the metal salt film would be destroyed and afterwards the pit bottom will be salt film free. This event results in an ohmic/activation control regime to be established [51]. In this region, current density decreases linearly with potential. The current density at which diffusion control dissolution is disrupted corresponds to C_S and is called limiting current density (i_{lim}). At this stage, pit still continues to grow until the composition of the pit electrolyte is such that repassivation is possible. By lowering the potential, the metal ions concentration reduces to a value below the critical concentration of cations necessary to stable pit growth (C^*) and thereby repassivation occurs.

Combination of Eqs. (1) and (2) leads to the linear relation between second power of pit depth and time (Eq. (3)) indicating that in diffusional controlled condition.

$$\delta^2 = \frac{M_w \cdot D \cdot C_S}{\rho} \times t \tag{3}$$

Fig. 8 depicts the variation of δ^2 against time extracted from the plateau region of Fig. 7. It can be seen that the square of pit depth increases linearly with time, which confirms the existence of diffusion controlled regime in the plateau region. Furthermore, assuming identical values of M_w and ρ for all samples with different solution annealing treatments, the slope of variation of δ^2 against t is proportion to $D \cdot C_S$. The decreased slope attributed to the alloy solution annealed at 1250 °C implies that compared to the alloy solution annealed at 1050 °C, the value of DC_S is lower in sample solution annealed at 1250 °C.

Fig. 9 compares the limiting current densities (i_{lim}) of solution annealed samples at various pit depths. The current density at the potential which salt film was dissolved is considered as the limiting current density. In the range of calculated pit depth

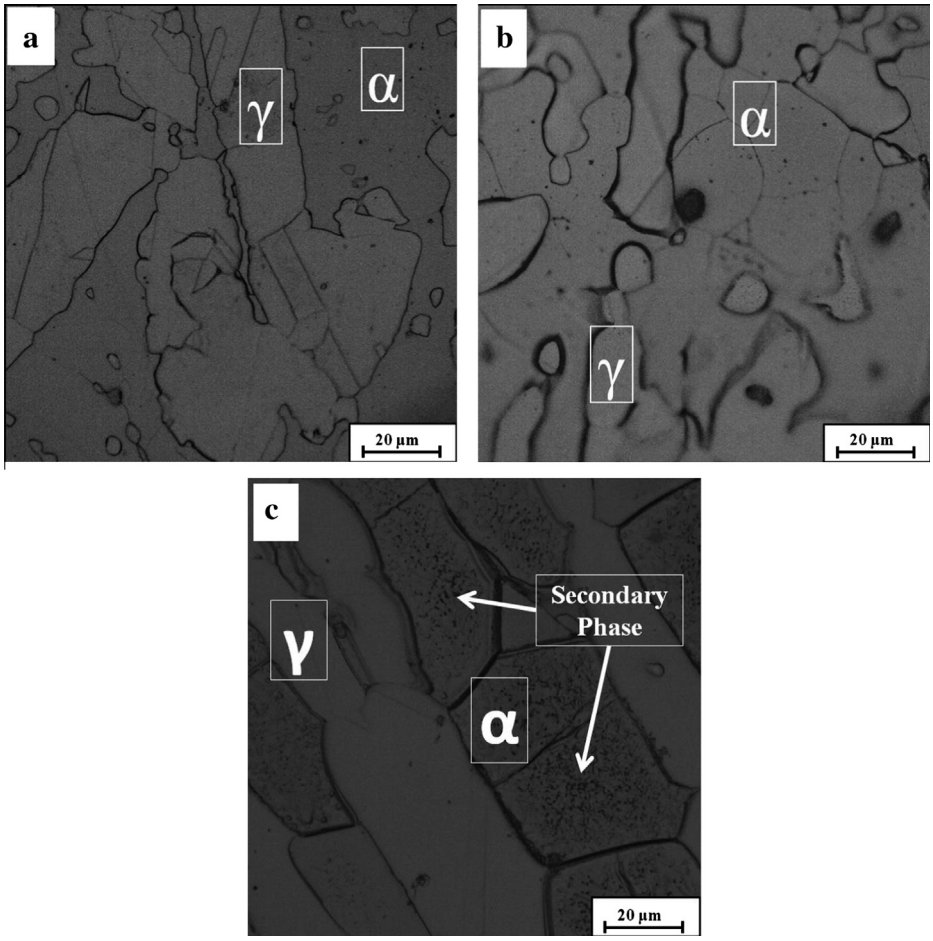

Fig. 2. Optical micrographs of DSS 2205 solution annealed at (a) 1050 °C, (b) 1150 °C, and (c) 1250 °C, etched in glyceregia, showing no secondary phases in the microstructure of alloy solution annealed at 1050 °C and 1150 °C and being an evidence for the existence of the secondary phases in ferritic region in the microstructure of sample solution annealed at 1250 °C.

(540–720 µm), the value of i_{lim} is between 201 mA cm^{-2} and 224 mA cm^{-2} for the sample solution annealed at 1050 °C. In comparison, for sample solution annealed at 1250 °C, the value of i_{lim} was lower and was found to be in a value between 160 mA cm^{-2} and 178 mA cm^{-2}.

Obtained limiting current densities (shown in Fig. 9) were used for determination of the saturation concentration of cations in pit anolyte via Fick's first law (Eq. (1)). Considering the value of 10^{-5} cm^2 s^{-1} as the average diffusion coefficient [11,51] and based on the values of DC_S presented in Fig. 10, saturation concentration of alloy solution annealed at 1050 °C was between 5.7×10^{-3} mol cm^{-3} and 7×10^{-3} mol cm^{-3}, while the value of C_S was between 4.5×10^{-3} mol cm^{-3} and 5.4×10^{-3} mol cm^{-3} for sample solution annealed at 1250 °C.

3.3.2. Active pit dissolution

The effect of solution annealing temperature on active dissolution of DSS 2205 solution annealed at 1050 °C and 1250 °C was investigated by potentiodynamic examination in 5 M HCl media at various test temperatures using 200 µm pencil electrode. 5 M HCl medium with a high concentration of aggressive anions and with a very low pH (in a range of pH −0.13 and 0.80 [62]) is an appropriate choice for simulating the pit anolyte in initial stage of pitting. Because of high dissolution rate of alloy in this solution, a condition similar to pit environment is produced by metal cations in contact with the surface [58].

Typical anodic polarisation curves for alloy solution annealed at 1050 °C and 1250 °C at different temperatures are illustrated in Fig. 11a and b, respectively. Similar active dissolution kinetics with rather different maximum current density was observed for alloys in both solution annealing conditions. Current density response to the potential scanning at different temperatures are grouped into three categories. Active dissolution of samples followed by surface passivity is evident at temperatures below 55 °C. At temperature of 55 °C, a tendency to passivity is observable, however salt film precipitation leads to diffusion controlled dissolution. It can be seen that current density is under diffusion controlled at higher temperatures.

Each test was repeated at least five times and the average values of maximum current densities (i_{max}) were plotted vs. temperature (Fig. 12). At low temperatures, the i_{max} value of both alloys linearly increases with temperature. This trend is changed at temperature between 45 °C and 55 °C for sample solution annealed at 1050 °C, while the change in linear behaviour of i_{max} vs. time for sample solution annealed at 1250 °C happens at a temperature between 35 °C and 45 °C which implies to salt film precipitation. In fact, precipitation of salt prevents the current density to reach the maximum value at these temperatures. Therefore, the linear trends of i_{max} – temperature were extrapolated to higher temperatures for approximation of the maximum current density at elevated temperatures.

Comparing the results of maximum current densities depicted in Fig. 12, it is apparent that solution annealing at 1250 °C leads

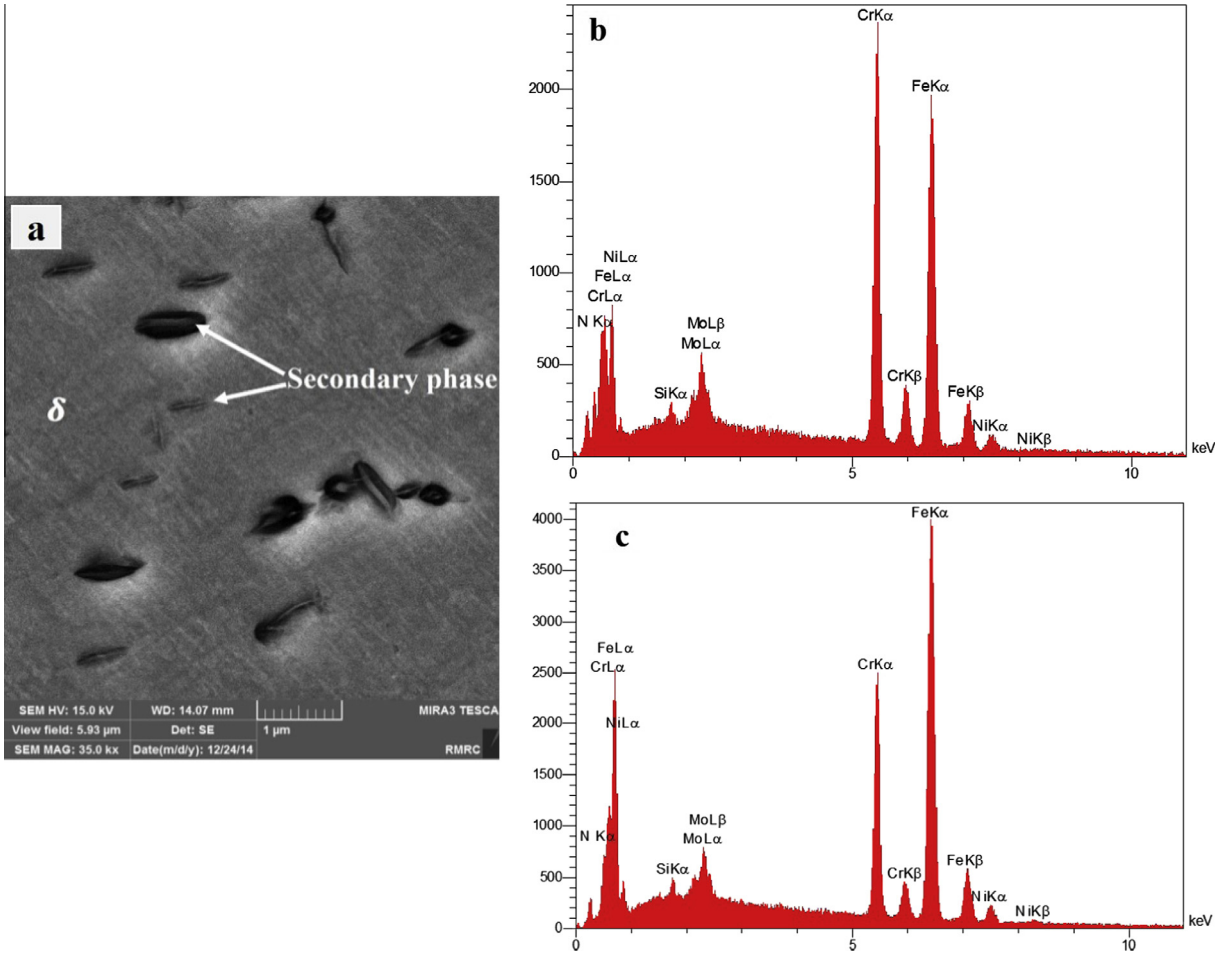

Fig. 3. (a) The SEM micrograph of sample solution annealed at 1250 °C. (b) The EDS spectra of the secondary phase. (c) The EDS spectra of the ferritic matrix.

to an increase in the value of maximum current density. In addition, in compare with alloy solution annealed at 1050 °C the slope of i_{max} vs. temperature curve for alloy solution annealed at 1250 °C is increased.

4. Discussion

The CPT measurement results showed that the CPT of alloy solution annealed at 1250 °C is reduced compared to others. However, no change was observed between the CPT of sample solution annealed at 1050 °C and sample solution annealed at 1150 °C. Since in both samples, the ferrite/austenite phase fraction is changed compared to the ferrite to austenite fraction obtained from sample solution annealed at 1050 °C, it cannot be claimed that the lower CPT of sample solution annealed at 1250 °C is directly related to the increase in ferrite/austenite proportion. Scanning electron microscopy revealed that chromium nitride phase are formed in the ferrite region in sample solution annealed at 1250 °C. Many researchers has identified the precipitation of chromium nitride phase during fast cooling from high temperatures in duplex stainless steels [23,25,35,38–40,53,63]. The only phase that is reported to be precipitated during non-isothermal treatment is the chromium nitride phase which called quenched-in nitrides [64]. They reported that no secondary phase is thermodynamically stable at temperatures above 1000 °C. When the ferrite content is high enough and cooling rate is too much for the nitrogen to reach austenite, due to difference in solubility of nitrogen in ferrite and austenite, the amount of nitrogen in ferrite exceeded the nitrogen solubility limit in this phase [23] and nitrogen has insufficient time to partition in the austenite, and consequently intense precipitation of chromium nitride occurs in the interior of the ferrite grains (in some distance from austenite) [65] as observed in the microstructures shown in Figs. 2c and 3.

The lower CPT for the alloy solution annealed at 1250 °C could be explained basically due to the presence of chromium nitride phase in the microstructure of alloy in this annealing condition. Deterioration in pitting corrosion resistance of 2205 DSS in presence of chromium nitride precipitation has been previously reported [40]. Chromium has the main role in passive layer formation in stainless steels [66]. Depletion of Cr in the region adjacent to chromium enriched particles can create an area with a weak passive layer [67,68] and consequently leads to the lower CPT of alloy rapid quenched from 1250 °C. In addition, secondary phases (considered as chromium nitride), could be as the active sites of pit initiation [25,53,54]. So, when alloy exposed to aggressive solutions, austenite/ferrite interfaces acts as the preferential sites for pit initiation. Thus, both pitting corrosion resistance and CPT of 2205 alloy decreases due to precipitation of chromium and nitrogen rich phase through solution annealing at 1250 °C. Furthermore, in literature, the effect of solution annealing temperature on the CPT was explained based on the PREN (pitting resistance equivalent number) of phases. It is reported that PREN of the ferrite phase decreases with the increase in the solution annealing temperature due to the uneven partitioning of alloying elements between ferrite and austenite phase [23,25,69]. Since the weaker phase controls the alloy susceptibility to pitting corrosion, ferrite phase of alloy subjected to high solution annealing

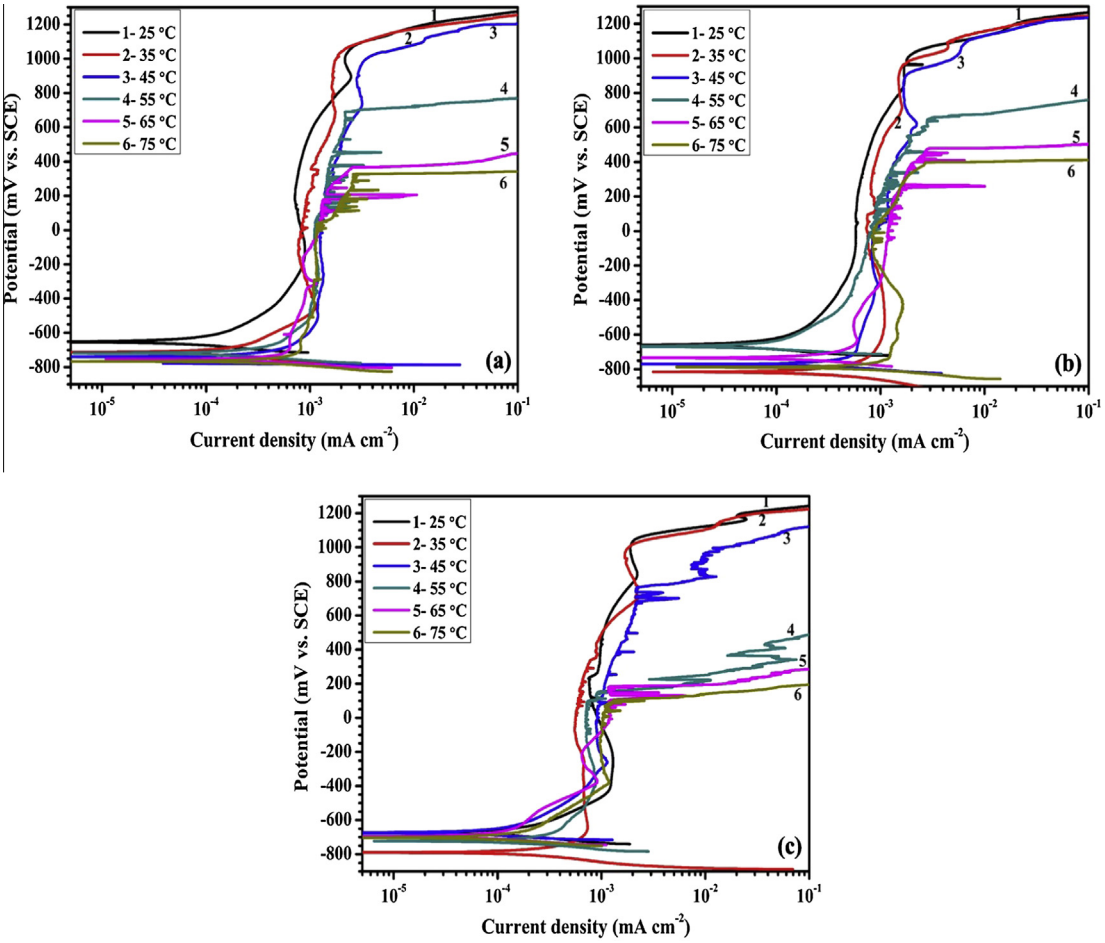

Fig. 4. Potentiodynamic polarisation curves of DSS 2205 solution annealed at (a) 1050 °C, (b) 1150 °C, (c) 1250 °C, in 3.5 wt.% NaCl solution at different test temperatures. Potential sweep rate was 0.5 mV s^{-1}.

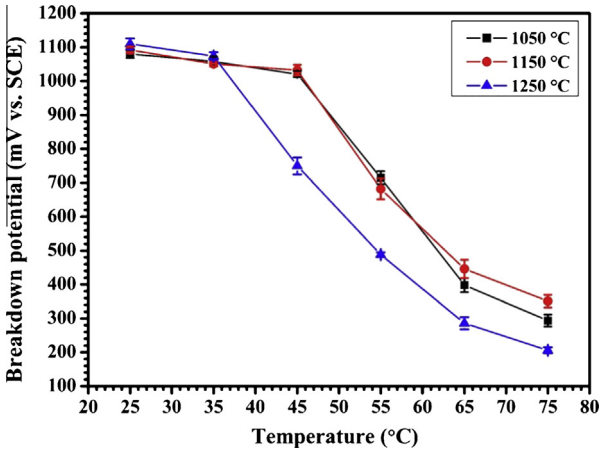

Fig. 5. Breakdown potentials against temperature for DSS 2205 solution annealed at various temperatures, obtained from the potentiodynamic polarisation in 3.5 wt.% NaCl solution. Potential sweep rate was 0.5 mV s^{-1}.

temperatures becomes the preferential phase to pit initiation. Subsequently, the pitting corrosion occurs at lower temperatures (i.e. lower CPT). However, the calculation of PREN and the relation between CPT and PREN was not interested in this research.

Pencil electrode studies were performed in 3.5 wt.% NaCl solution at 65 °C to understand how pit chemistry alters due to solution annealing.

Once single pit is created due to the coalesce of small pits generated on the pencil electrode surface, the current density begins to decrease as a result of salt precipitation at the pit bottom and then becomes under the diffusion controlled of the metal cations dissolving through the metal salt. The results obtained from pencil electrode studies revealed that for sample solution annealed at 1250 °C, the limiting current density (i_{lim}) and correspondingly the saturation concentration of metal cations essential for the metal salt to precipitate at the pit bottom (C_S) is lower in comparison to the sample subjected to 1050 °C.

A probable explanation for lower saturated concentration of alloy solution annealed at 1250 °C could be based on the presence of chromium and nitrogen rich secondary phase in the microstructure of alloy in this annealing condition. Since chromium nitride is practically noble compare to surrounding phases in duplex stainless steel [70], so it can be concluded that, this phase would not be dissolved during the metal cations dissolution and will enter to the pit solution in undissolved form. This is the outer opinion that the presence of chromium nitride in solid form in the pit media could facilitate the metal salt precipitation due to the increase in the preferential sites for metal salt to precipitate. Thus, it can be concluded that salt precipitation at the pit bottom can occur at the lower metal cations concentrations. In other words, the saturation concentration of metal cations essential for salt to precipitate at the pit bottom (C_S) is decreased for specimen solution annealed at 1250 °C. The other possible reason should leis on the change of salt film composition at the pit bottom. However, the metal salt composition precipitated at the pit bottom formed on the stainless steels

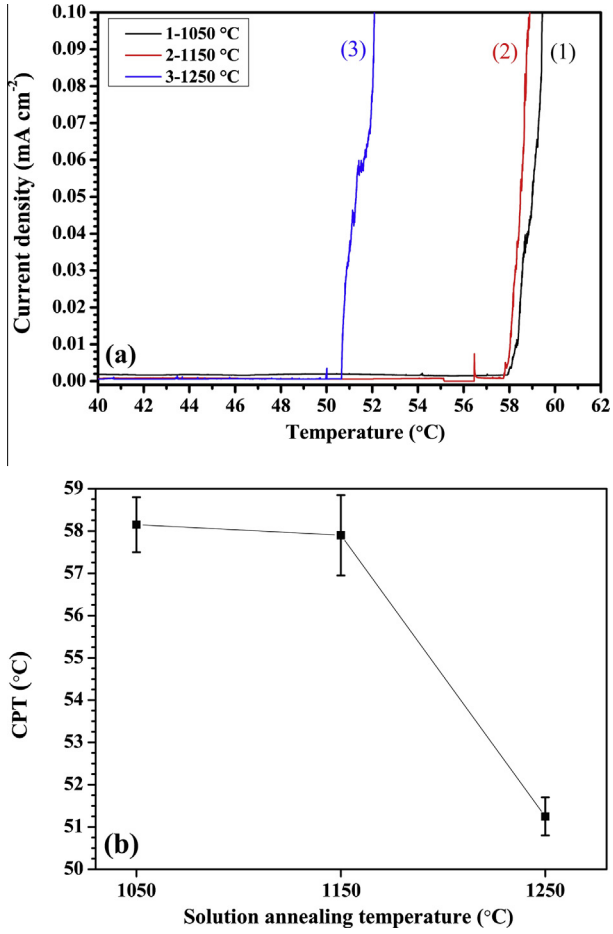

Fig. 6. The results of the evaluation of CPT of DSS 2205 by potentiostatic measurement at 750 mV (SCE) in 3.5 wt.% NaCl solution and temperature increasing rate of 0.6 °C min^{-1}. (a) Typical current density vs. time and (b) the values of critical pitting temperature of DSS 2205 as a function of solution annealing temperature. (Error bars show 95% confidence limit.)

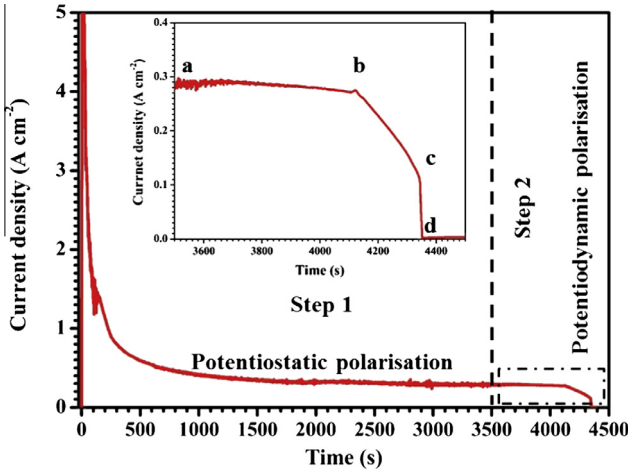

Fig. 7. Typical current density vs. time curve of 80 μm dia. pencil electrode (made from a DSS 2205 wire which was solution annealed at 1050 °C) in 3.5 wt.% NaCl solution at 65 °C, showing two steps of experiments (step 1: potentiostatic polarisation at 850 mV (SCE) and step 2: potentiodynamic polarisation at a sweep rate of −1 mV s^{-1}).

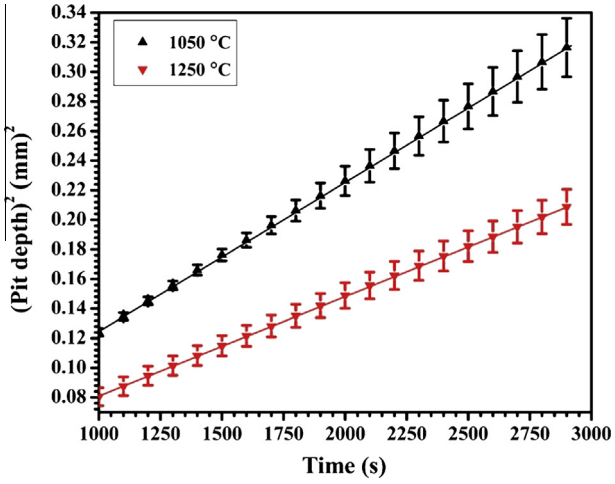

Fig. 8. Square of pit depth vs. time obtained from potentiostatic polarisation test results for 80 μm dia. DSS 2205 pencil electrode in 3.5 wt.% NaCl solution at 850 mV (SCE) at 65 °C. Error bars show 95% confidence limit.

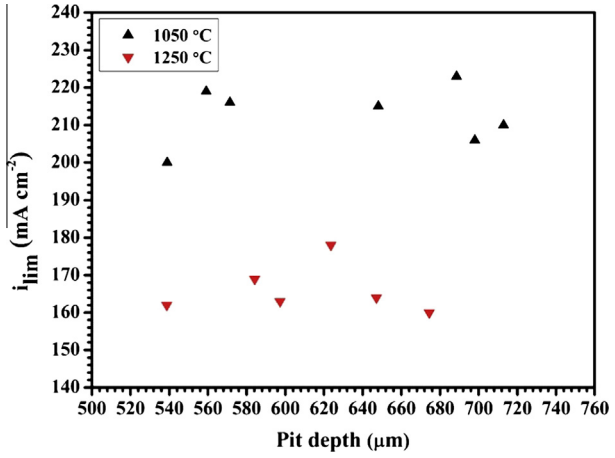

Fig. 9. Diffusion controlled limiting current density (i_{lim}) as a function of pit depth obtained from tests conducted in 3.5 wt.% NaCl solution at 65 °C using 80 μm dia. DSS 2205 pencil electrodes.

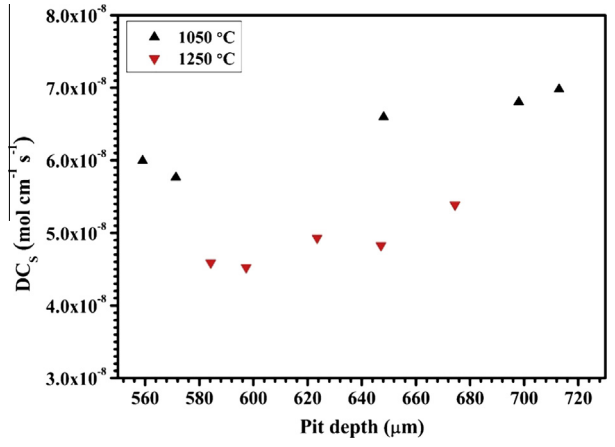

Fig. 10. The values of $D \cdot C_S$ as a function of pit depth obtained from test conducted in 3.5 wt.% NaCl solution at 65 °C using 80 μm dia. DSS 2205 pencil electrodes.

have been considered as $FeCl_2$ [11,19,49,51], but investigation of corrosion product during pitting of Fe–Cr–Ni alloys has shown that all three Cr, Ni and Fe are presence in metal salt precipitated at the pit bottom in their stoichiometric proportion existed in the bulk alloy [18]. On the basis that chromium nitride is a Cr rich phase and does not dissolve during pit dissolution, the presence of this

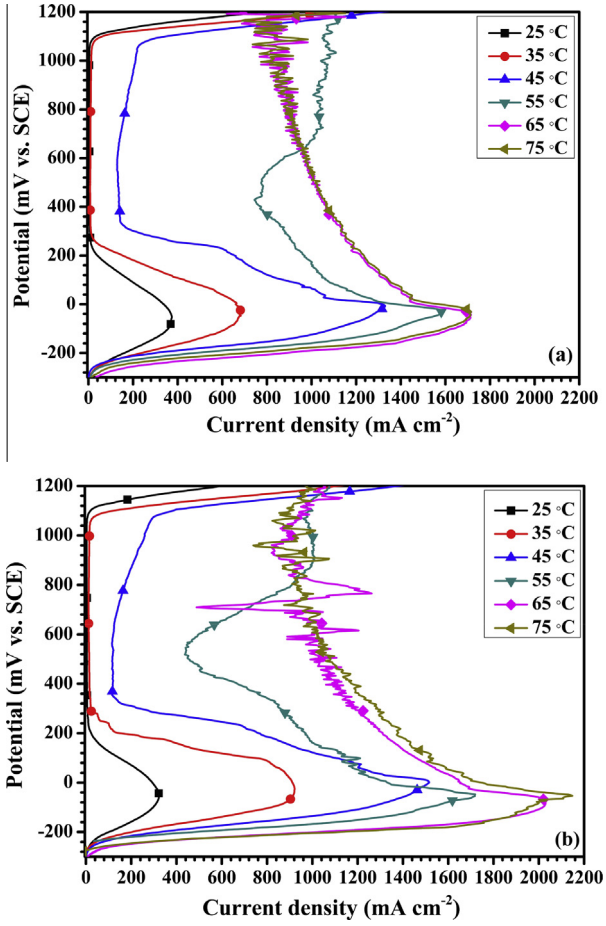

Fig. 11. Typical potentiodynamic polarisation curves for 200 μm dia. DSS 2205 pencil electrode solution annealed at (a) 1050 °C, and (b) 1250 °C in 5 M HCl solution at various tem. Scan rate was 5 mV s^{-1}.

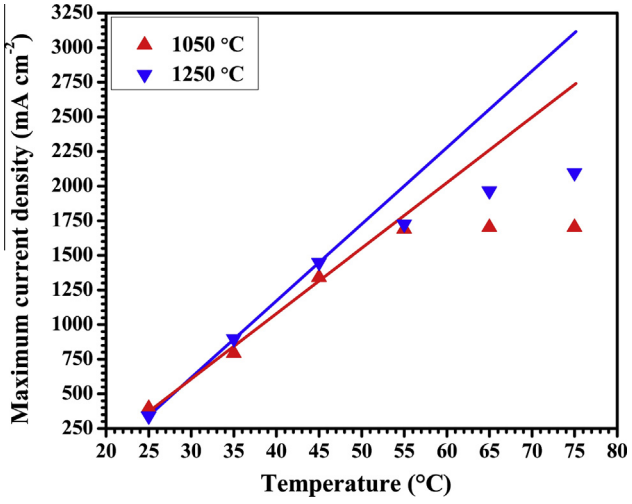

Fig. 12. Maximum current density as a function of temperature obtained from potentiodynamic polarisation curves of DSS 2205 at different solution annealing conditions, solid lines show the best trend fits and broken lines represent extrapolated data.

phase could lead to a decrease in the chromium percentage involved in dissolution and decreases the proportion of chromium chloride in the metal salt composition. Thus, the metal cations concentration required for a salt to precipitate is decreased and consequently salt precipitation would be facilitated. However, further investigation

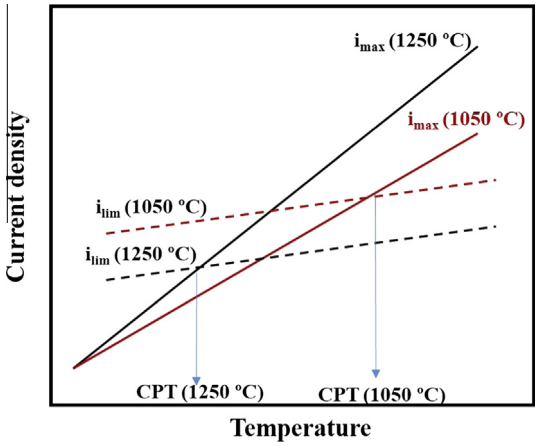

Fig. 13. Schematic graph representing i_{lim} and i_{max} vs. temperature, effect of decreasing the limiting current density and increasing the critical current density on deterioration of CPT in DSS 2205 solution annealed at 1050 °C in comparison to alloy solution annealed at 1250 °C is represented.

on the composition of salt film is required to prove the mechanism involved.

Based on the CPT definition proposed by Salinas-Bravo and Newman (i.e. the temperature at which the limiting current density equals the critical current density essential for passivity in the pit solution) [45] and ignoring the effect of maximum current density within the pit, a decrease in the value of i_{lim} due to solution annealing at 1250 °C, leads to a decrease in CPT.

For alloy subjected to 1250 °C, the maximum current density in simulated pit solution shown to be increased with test solution temperature more rapidly than alloy which was solution annealed at 1050 °C. Higher maximum current density of alloy in this solution annealing condition is possibly attributed to precipitation of the secondary phase in the alloy microstructure. As discussed above, chromium depletion occurred due to the secondary phase precipitation, leads to a decrease in corrosion resistance at the vicinity of chromium rich precipitates. In addition, the secondary phase precipitates, act as preferential sites for pits initiation. Thus, maximum current density which is required to ban active dissolution and to passive active sites is reasonable to increase in presence of this phase.

Based on CPT theory introduced by Salinas-Bravo and Newman [45], an increase in maximum current density aside of the effect of i_{lim} could be the reason of decreased CPT of 2205 duplex stainless steel solution annealed at 1250 °C.

Because reproducible data was hard to reach at higher temperatures, considering the same increasing trend of diffusion controlled limiting current density (i_{lim}) with temperature, schematic diagram screening i_{lim} and i_{max} as functions of temperature is illustrated in Fig. 13 to understand how changes in value of i_{lim} and i_{max} due to the solution annealing effect on the CPT value [45].

The results lead to the conclusion that by solution annealing at 1250 °C, the intersection point of i_{lim} and i_{max} (CPT) moves backward respect to another one, and thus, the value of CPT decreases due to the setback moving of this cross section.

5. Conclusion

The correlation between critical pitting temperature and pit chemistry of 2205 duplex stainless steel solution annealed at different temperatures was investigated applying electrochemical evaluations and pencil electrode studies. The results summarised as below:

1. Potentiodynamic measurements in 3.5 wt.% NaCl solution showed that CPT of DSS 2205 solution annealed at 1050 °C and 1150 °C is a temperature between 45 °C and 55 °C (not necessarily a same temperature). It was revealed that this temperature is decreased to a value between 35 °C and 45 °C for sample solution annealed at 1250 °C. The CPT values obtained from potentiostatic polarisation experiments were consistent with potentiodynamic polarisation results. These experiments revealed that subjecting to 1250 °C, leads to almost 7 °C decrease in the CPT of 316 SS.
2. Pencil electrode results revealed that in comparison with sample solution annealed at 1050 °C, the value of diffusion controlled limiting current density (i_{lim}) and saturation concentration of metal cations necessary for the metal salt to precipitate at the pit bottom (C_S) is lower for sample solution annealed at 1250 °C.
3. Potentiodynamic polarisation in simulated pit solution (5 M HCl media) revealed that the maximum current density within the pit solution (i_{max}) is higher for alloy solution annealed at 1250 °C.
4. The experimental results support the CPT model suggested by Salinas-Bravo and Newman. The lower CPT of alloy solution annealed at 1250 °C is explained by a decrease in the temperature at which the limiting current density and the maximum current density are equal.

Acknowledgment

Ferdowsi University of Mashhad (FUM)/Iran is gratefully appreciated for financial support and providing laboratory facilities.

References

[1] J.R. Galvele, Transport processes and the mechanism of pitting of metals, J. Electrochem. Soc. 123 (1976) 464–474.
[2] Y. Zuo, H. Wang, J. Zhao, J. Xiong, The effects of some anions on metastable pitting of 316L stainless steel, Corros. Sci. 44 (2002) 13–24.
[3] J. Mankowski, Z. Szklarska-Smialowska, Studies on accumulation of chloride ions in pits growing during anodic polarization, Corros. Sci. 15 (1975) 493–501.
[4] J. Horvath, H.H. Uhlig, Critical potentials for pitting corrosion of Ni, Cr–Ni, Cr–Fe and related stainless steels, J. Electrochem. Soc. 115 (1968) 791–795.
[5] J.R. Galvele, Pitting corrosion, in: J.C. Scully (Ed.), Treatise on Materials Science and Technology, Academic Press, New York, 1983, pp. 1–53.
[6] R.C. Alkire, K.P. Wong, The corrosion of single pits on stainless steel in acidic chloride solution, Corros. Sci. 28 (1988) 411–421.
[7] R.C. Alkire, M. Feldman, Initiation of single corrosion pits on pure aluminum by focused laser radiation, J. Electrochem. Soc. 135 (1988) 1850–1851.
[8] G. Wranglen, Pitting and sulphide inclusions in steel, Corros. Sci. 14 (1974) 331–349.
[9] J.H. Wang, C.C. Su, Z. Szklarska-Smialowska, Effects of Cl^- concentration and temperature on pitting of AISI 304 stainless steel, Corrosion 44 (1988) 732.
[10] H.S. Isaacs, G. Kissel, Surface preparation and pit propagation in stainless steels, J. Electrochem. Soc. 119 (1972) 1628–1632.
[11] P.C. Pistorius, G.T. Burstein, Metastable pitting corrosion of stainless steel and the transition to stability, Philos. Trans. R. Soc. London, A 341 (1992) 531–559.
[12] T.R. Beck, R.C. Alkire, Occurrence of salt films during initiation and growth of corrosion pits, J. Electrochem. Soc. 126 (1979) 1662–1666.
[13] H.S. Isaacs, The behavior of resistive layers in the localized corrosion of stainless steel, J. Electrochem. Soc. 120 (1973) 1456.
[14] R.C. Newman, H.S. Isaacs, Diffusion coupled active dissolution in the localized corrosion of stainless steels, J. Electrochem. Soc. 130 (1983) 1621–1624.
[15] R.C. Newman, H.S. Isaacs, Passivity of metals and semiconductors, in: M. Froment (Ed.), 5th International Symposia of Passivity, Elsevier, Amsterdam, 1983, pp. 269–274.
[16] J.W. Tester, H.S. Isaacs, Diffusional effects in simulated localized corrosion, J. Electrochem. Soc. 122 (1975) 1438–1445.
[17] V.M. Novakovski, A.N. Sorokina, Model study of chloride pitting in 18-8 stainless steel, Corros. Sci. 6 (1966) 227–233.
[18] H.S. Isaacs, J.-H. Cho, M.L. Rivers, S.R. Sutton, In situ X-ray microprobe study of salt layers during anodic dissolution of stainless steel in chloride solution, J. Electrochem. Soc. 142 (1995) 1111–1118.
[19] T. Rayment, A.J. Davenport, A.J. Dent, J.-P. Tinnes, R.J.K. Wiltshire, C. Martin, G. Clark, P. Quinn, J.F.W. Mosselmans, Characterisation of salt films on dissolving metal surfaces in artificial corrosion pits via in situ synchrotron X-ray diffraction, Electrochem. Commun. 10 (2008) 855–858.
[20] H.S. Isaacs, S.M. Huang, Behavior of dissolved molybdenum during localized corrosion of austenitic stainless steel, J. Electrochem. Soc. 143 (1996) L277–L279.
[21] R.J. Brigham, E.W. Tozer, Temperature as a pitting criterion, Corrosion 29 (1973) 33–36.
[22] R.J. Brigham, E.W. Tozer, Effect of alloying additions on the pitting resistance of 18% Cr austenitic stainless steel, Corrosion 30 (1974) 161–166.
[23] L. Zhang, W. Zhang, Y. Jaiang, B. Deng, D. Sun, J. Li, Influence of annealing treatment on the corrosion resistance of lean duplex stainless steel 2101, Electrochim. Acta 54 (2009) 5387–5392.
[24] A.M. do Nascimento, M.C.F. Ierardi, A.Y. Kina, S.S.M. Tavares, Pitting corrosion resistance of cast duplex stainless steels in 3.5%NaCl solution, Mater. Charact. 59 (2008) 1736–1740.
[25] B. Deng, Y.M. Jiang, J. Gao, J. Li, Effect of annealing treatment on microstructure evolution and the associated corrosion behavior of a super-duplex stainless steel, J. Alloy. Compd. 493 (2010) 461–464.
[26] N. Ebrahimi, M.H. Moayed, A. Davoodi, Critical pitting temperature dependence of 2205 duplex stainless steel on dichromate ion concentration in chloride medium, Corros. Sci. 53 (2011) 1278–1287.
[27] B. Deng, Y. Jiang, J. Gong, C. Zhong, J. Gao, J. Li, Critical pitting and repassivation temperatures for duplex stainless steel in chloride solutions, Electrochim. Acta 53 (2008) 5220–5225.
[28] Practical Guidelines for the Fabrication of Duplex Stainless Steels, Contributors International Molybdenum Association, International Molybdenum Association Staff, TMR Stainless (Firm), TMR Stainless (Firm) Staff Edition 2, 2009.
[29] K. Vijayalakshmi, V. Muthupandi, R. Jayachitra, Influence of heat treatment on the microstructure, ultrasonic attenuation and hardness of SAF 2205 duplex stainless steel, Mater. Sci. Eng. A 529 (2011) 447–451.
[30] H. Tan, Y. Jiang, B. Deng, T. Sun, J. Xu, J. Li, Effect of annealing temperature on the pitting corrosion resistance of super duplex stainless steel UNS S32750, Mater. Charact. 60 (2009) 1049–1054.
[31] Y. Yang, H. Tan, Z. Zhang, Z. Wang, Y. Jiang, L. Jiang, J. Li, Effect of annealing temperature on the pitting corrosion behavior of UNS S82441 duplex stainless steel, Corrosion 69 (2012) 167–173.
[32] D.H. Kang, H.W. Lee, Study of the correlation between pitting corrosion and the component ratio of the dual phase in duplex stainless steel welds, Corros. Sci. 74 (2013) 396–407.
[33] Y. Yang, B. Yan, J. Li, J. Wang, The effect of large heat input on the microstructure and corrosion behaviour of simulated heat affected zone in 2205 duplex stainless steel, Corros. Sci. 53 (2011) 3756–3763.
[34] Y. Jiang, H. Tan, Z. Wang, J. Hong, L. Jiang, J. Li, Influence of Cr eq/Ni eq on pitting corrosion resistance and mechanical properties of UNS S32304 duplex stainless steel welded joints, Corros. Sci. 70 (2013) 252–259.
[35] E. Angelini, B. De Benedetti, F. Rosalbino, Microstructural evolution and localized corrosion resistance of an aged superduplex stainless steel, Corros. Sci. 46 (2004) 1351–1367.
[36] B. Deng, Z.Y. Wang, Y.M. Jiang, H. Wang, J. Gao, J. Li, Evaluation of localized corrosion in duplex stainless steel aged at 850 °C with critical pitting temperature measurement, Electrochim. Acta 54 (2009) 2790–2794.
[37] N. Ebrahimi, M. Momeni, M.H. Moayed, A. Davoodi, Correlation between critical pitting temperature and degree of sensitisation on alloy 2205 duplex stainless steel, Corros. Sci. 43 (1987) 637–644.
[38] J.C. Lippold, D.J. Kotecki, in: Damian J. Kotecki (Ed.), Welding Metallurgy and Weldability of Stainless Steels, Wiley-Interscience, 2005.
[39] R.A. Perren, T.A. Suter, C. Solenthaler, G. Gullo, P.J. Uggowitzer, H. Böhni, M.O. Speidel, Corrosion resistance of super duplex stainless steels in chloride ion containing environments: investigations by means of a new microelectrochemical method: II. Influence of precipitates, Corros. Sci. 43 (2001) 727–745.
[40] V.S. Moura, L.D. Lima, J.M. Pardal, A.Y. Kina, R.R.A. Corte, S.S.M. Tavares, Influence of microstructure on the corrosion resistance of the duplex stainless steel UNS S31803, Mater. Charact. 59 (2008) 1127–1132.
[41] G.S. Frankel, L. Stockert, F. Hunkeler, H. Boehni, Metastable pitting of stainless steel, Corrosion 43 (1987) 429–436.
[42] L.F. Garfias-Mesias, J.M. Sykes, C.D.S. Tuck, The effect of phase compositions on the pitting corrosion of 25 Cr duplex stainless steel in chloride solutions, Corros. Sci. 38 (1996) 1319–1330.
[43] R. Ovarfort, Critical pitting temperature measurements of stainless steels with an improved electrochemical method, Corros. Sci. 29 (1989) 987–993.
[44] R.C. Newman, E.M. Franz, Growth and repassivation of single corrosion pits in stainless steel, Corrosion 40 (1984) 325–330.
[45] V.M. Salinas-Bravo, R.C. Newman, An alternative method to determine critical pitting temperature of stainless steels in ferric chloride solution, Corros. Sci. 36 (1994) 67–77.
[46] M.H. Moayed, N.J. Laycock, R.C. Newman, Dependence of the critical pitting temperature on surface roughness, Corros. Sci. 45 (2003) 1203–1216.
[47] M.H. Moayed, R.C. Newman, Deterioration in critical pitting temperature of 904L stainless steel by addition of sulfate ions, Corros. Sci. 48 (2006) 3513–3530.
[48] M. Naghizadeh, D. Nakhaie, M. Zakeri, M.H. Moayed, Effect of thiosulfate on pitting corrosion of 316SS: I. Critical pitting temperature and pit chemistry, J. Electrochem. Soc. 162 (2015) C71–C77.
[49] M. Zakeri, M.H. Moayed, Investigation on the effect of nitrate ion on the critical pitting temperature of 2205 duplex stainless steel along a mechanistic approach using pencil electrode, Corros. Sci. 85 (2014) 222–231.

[50] P. Ernst, R.C. Newman, Pit growth studies in stainless steel foils. I. Introduction and pit growth kinetics, Corros. Sci. 44 (2002) 927–941.
[51] P. Ernst, R.C. Newman, Pit growth studies in stainless steel foils. II. Effect of temperature, chloride concentration and sulphate addition, Corros. Sci. 44 (2002) 943–954.
[52] P. Ernst, R.C. Newman, Explanation of the effect of high chloride concentration on the critical pitting temperature of stainless steel, Corros. Sci. 49 (2007) 3705–3715.
[53] B. Deng, Z. Wang, Y. Jiang, T. Sun, J. Xu, J. Li, Effect of thermal cycles on the corrosion and mechanical properties of UNS S31803 duplex stainless steel, Corros. Sci. 51 (2009) 2969–2975.
[54] H.-Y. Liou, R.-I. Hsieh, W.-T. Tsai, Microstructure and pitting corrosion in simulated heat-affected zones of duplex stainless steels, Mater. Chem. Phys. 74 (2002) 33–42.
[55] B. Bramfitt, Metallographer's Guide Practices and Procedures for Irons and Steels, ASM International, 2002.
[56] F. Eghbali, M.H. Moayed, A. Davoodi, N. Ebrahimi, Critical pitting temperature (CPT) assessment of 2205 duplex stainless steel in 0.1 M NaCl at various molybdate concentrations, Corros. Sci. 53 (2011) 513–522.
[57] L. Peguet, A. Gaugain, C. Dussart, B. Malki, B. Baroux, Statistical study of the critical pitting temperature of 22-05 duplex stainless steel, Corros. Sci. 60 (2012) 280–283.
[58] R.C. Newman, T. Shahrabi, The effect of alloyed nitrogen or dissolved nitrate ions on the anodic behaviour of austenitic stainless steel in hydrochloric acid, Corros. Sci. 27 (1987) 827–838.
[59] A. Neville, T. Hodgkiess, An assessment of the corrosion behaviour of highgrade alloys in seawater at elevated temperature and under a high velocity impinging flow, Corros. Sci. 38 (1996) 927–956.
[60] R.C. Newman, M.A.A. Ajjawi, A micro-electrode study of the nitrate effect on pitting of stainless steels, Corros. Sci. 26 (1986) 1057–1063.
[61] H.S. Isaacs, R.C. Newman, in: R.P. Frankenthal, F. Mansfeld (Eds.), Corrosion and Corrosion Protection, The Electrochemical Society Proceedings Series, Pennington, NJ, 1981, p. 120.
[62] T. Suzuki, M. Yamabe, Y. Kitamura, Composition of pit anode within pit anode of austenitic stainless steels in chloride solutions, Corrosion 29 (1973).
[63] H. Ha, H. Kwon, Effects of Cr_2N on the pitting corrosion of high nitrogen stainless steels, Electrochim. Acta 52 (2007) 2175–2180.
[64] U.K.E. Bettini, C. Leygraf, J. Pan, Study of corrosion behavior of a 2507 super duplex stainless steel: influence of quenched-in and isothermal nitrides, Int. J. Electrochem. Sci. 9 (2014) 61–80.
[65] A.J. Ramirez, J.C. Lippold, S.D. Brandi, The relationship between chromium nitride and secondary austenite precipitation in duplex stainless steels, Metall. Mater. Trans. A 34A (2003) 1597.
[66] E.E. Stansbury, R.A. Buchanan, Fundamentals of Electrochemical Corrosion, ASM International, Materials Park, OH, 2000.
[67] L.R. Scharfstein, Effects of composition, structure and heat treatment on the corrosion resistance of stainless steel, in: D. Peckner, I.M. Bernstein (Eds.), Handbook of Stainless Steels, McGraw-Hill, 1977.
[68] Z.L. Zhang, T. Bell, Structure and corrosion resistance of plasma nitrided stainless steel, Surf. Eng. 1 (1985) 131–136.
[69] R.A. Perren, T.A. Suter, L. Weber, R. Magdowski, H. Böhni, M.O. Speidel, Corrosion resistance of super duplex stainless steels in chloride ion containing environments: investigations by means of a new microelectrochemical method I. Precipitation-free states, Corros. Sci. 43 (2001) 707–726.
[70] N. Sathirachinda, R. Pettersson, S. Wessman, J. ShanPan, Study of nobility of chromium nitrides in isothermally aged duplex stainless steels by using SKPFM and SEM/EDS, Corros. Sci. 52 (2010) 179–186.